Three new bismuth(III) pyridine-2,6-dicarboxylate compounds: Synthesis, characterization and crystal structures

Mohammad Hakimi, Elham Motieiyan, Federica Bertolotti, Domenica Marabello, Vitor Hugo Nunes Rodrigues, Three new bismuth(III) pyridine-2,6-dicarboxylate compounds: Synthesis, characterization and crystal structures", *Journal of Molecular Structure* **1099**, 5 (2015), 523-533, DOI: 10.1016/j.molstruc.2015.06.084

Three new bismuth(III) pyridine-2,6-dicarboxylate compounds: Synthesis, characterization and crystal structures

Mohammad Hakimi [a, *], Elham Motieiyan [a], Federica Bertolotti [b], Domenica Marabello [b], Vitor Hugo Nunes Rodrigues [c]

[a] Department of Chemistry, Payame Noor University, 19395e4697 Tehran, Iran

[b] Dipartimento di Chimica e Centro CrisDi, University of Turin, Via P. Giuria 7, 10125, Torino, Italy

[c] CFisUC, Department of Physics, Universidade de Coimbra, Rua Larga, 3004-516 Coimbra, Portugal

Keywords:
Bismuth, Anionic metal organic compounds, Hydrogen bonding networks, Proton transfer, X-ray crystal structure

abstract

Three new metal-organic compounds containing bismuth and pyridine-2,6-dicarboxylate (pydc) formulated as $(2\text{-apyH})_2[Bi(pydc)_2(pydcH)]\$2H_2O$, 1, $(4\text{-apyH})[Bi(pydc)(pydcH)_2].4H_2O$, 2 and (pipzeaH) $[Bi_2(pydc)_3(pydcH)(H_2O)_2]\$5H_2O$, 3, (2-apy ¼ 2-aminopyridine, 4-apy ¼ 4-aminopyridine, pipzea ¼ 2-piperazin-1-ylethanamine), have been synthesized in deionized water and characterized by elemental analysis (C, H and N), spectral (UVeVis, IR), ^{1}H NMR spectroscopy, TGA and single crystal X-ray diffraction. These compounds were obtained via proton transfer methodology. Compounds 1 and 2 have similar monomeric bismuth coordination units, whereas compound 3 has a dimeric bismuth coordination unit. The compounds are anionic in 1 and 2 and they are connected non-covalently to 2-apyH and 4-apyH, respectively. In 3, two molecules are present, one neutral and one anionic, and both are connected non-covalently to pipzeaH cations. Five different coordination modes of Bi-pydc exist in 1, 2 and 3. These compounds are stabilized in the solid state by a complex network of hydrogen bonds between crystal-lization water molecules, anionic, cationic and neutral fragments, forming 3D-supramolecular arrays.

1. Introduction

Design and construction of metaleorganic compounds, have been studied for a variety of potential applications [1,7]. Metal-eorganic compounds containing carboxylic acid ligands in combi-nation with transition metal and lanthanide ions have been studied extensively [8,11], but compounds based on s- and p-block metal ions have obtained popularity only in the recent past [12,18].

Pyridine-2,6-dicarboxylic acid, $pydcH_2$ is a versatile chelating ligand, with a recognized biological function in the body metabo-lisms [19], and in a variety of processes such as enzyme inhibitors, plant preservatives [20] and food sanitizers [21]. The complexation of metal ions with $pydcH_2$ has been the subject of numerous re-ports [9,10,22,29]. The reasons for this interest are the ability of the ligand to give stable chelates with different coordination modes [22], and its biological activity in human metabolisms [30]. Pyri-dine-2,6-dicarboxylate complexes have been used as electron carriers in some model biological systems as specific molecular tools in DNA cleavage [31] and as NO scavengers [32].

Bismuth-based materials have many potential applications in the field of photoluminescence, medicine, catalysis and piezoelec-tric or high dielectric constant materials [33,44]. A large number of bismuth(III) carboxylates are clinically active against Helicobacter pylori and other gastrointestinal disorders [35,44]. The bismuth(III) center is highly acidic and can exhibit variable coordination numbers, framework flexibilities, and different structural charac-teristics [16,18,34,51]. Bismuth(III) is known to form stable chelate complexes with $pydcH_2$ (or its anions) and various crystal struc-tures have been reported [16,17,45,51].

In order to gain more information about packing features of molecules containing bismuth(III) chelates, we have studied the synthesis, characterization, spectroscopic and crystal structures of bismuth(III)epydc complexes with 2-apyH, 4-apyH, or pipzeaH cations. We succeeded in synthesizing and characterizing three new crystalline compounds: $(2\text{-apyH})_2[Bi(pydc)_2(pydcH)]\$2H_2O$, 1, $(4\text{-apyH})[Bi(pydc)(pydcH)_2]\$4H_2O$, 2 and $(pipzeaH)[Bi_2(pydc)_3(\text{-}pydcH)(H_2O)_2]\$5H_2O$, 3. Compounds 1e3 are notable for several reasons. There is no report in the literature of any

$[Bi(pydc)_2(pydcH)]^2$, $[Bi(pydc)(pydcH)_2]$,$[Bi_2(pydc)_4(H_2O)_2]^2$ and $[Bi_2(pydc)_2(pydH)_2(H_2O)_2]$ complexes with $2\text{-apyH}^þ$, $4\text{-apyH}^þ$ and $pipzeaH^þ$ as counter ions. Moreover, four different coordina-tion modes of metal-dipicolinate (Scheme 1) exist in 1, 2 and 3, a rare coordination type in the bismuth dipicolinate complexes, (b) [13], and the other, (c), which has not been reported in the bismuth dipicolinate complexes.

2. Experimental setup

2.1. Reagents and apparatus

$Bi(NO_3)_3\$5H_2O$ (Aldrich, 98%), pyridine-2,6-dicarboxylic acid ($pydcH_2$) (Merck, 97%),2-apy ¼ 2-aminopyridine (Aldrich, 99%), 4-apy ¼ 4-aminopyridine (Aldrich, 98%) and pipzea ¼ 2-piperazin-1-ylethanamine (Merck, 97%) were used as purchased. Melting points were determined by applying a Barnstead

Electrothermal 9200 apparatus. Elemental analyses (C, H, and N) were performed with a Heraus CHN Pro apparatus. The IR spectroscopy was per-formed applying a Shimadzu 8400 Fourier transform spectropho-tometer (400e4000 cm ^{1}) using KBr disc. The NMR spectra were obtained applying a Bruker DRX 250 Avance spectrometer at 2500 MHz using d6-dimethylsulfoxide as solvent, chemical shifts are reported on the d scale relative to TMS (Scheme S1 and Figs. S1,S3). Thermogravimetric analysis (TGA) experiments were performed on a Netzsch TG 209 instrument at a heating rate of 10 C min ^{1}. Absorption spectra were recorded on a Shimadzu Model 160-A UVeVis spectrophotometer with a 1-cm quartz cell.

Suitable crystals of all the compounds were selected for crystal structure determination using single-crystal XRD. For 1 and 2, unit cell determination and full data collection were carried out on a Bruker APEX II diffractometer [52,53], while for compound 3, a Gemini R Ultra diffractometer [54] has been used, both equipped with a CCD area detector and a graphite monochromatized Mo-Ka radiation source. The multi-scan absorption correction has been applied for all the compounds. Data collection, reduction and ab-sorption correction were performed by the Bruker APEX II [53] software for complexes 1 and 2 and with CrisAlisPro [55] soft-ware for complex 3.

All structures were solved by direct methods and refined by full-matrix least-square on F^{2} using SHELX-97 package [56]. During structure refinements, all atoms (except H) have been refined anisotropically. For compound 1, 2 and 3, the hydrogen atoms of NH and NH_2 groups as well as the water molecules and H(O) were found in difference Fourier synthesis while the H(C) atom positions were calculated. All hydrogen atoms were refined with a riding model and $U_{iso}(H)$ parameters equal to $1.2U_{eq}(C_i)$, $1.2U_{eq}(N_i)$ and 1.2 or $1.5U_{eq}(O_i)$ where $U_{eq}(C_i)$, $U_{eq}(N_i)$, $U_{eq}(O_i)$ are respectively the equivalent thermal parameters of the carbon, nitrogen and oxygen atoms to which corresponding H atoms are bonded.

The molecular and crystal packing diagrams were generated using Mercury [57]. Geometrical calculations were done using PARST95 [58] present in the WinGX program suite [59].

Further details about data collections and refinements are reported in Table 1.

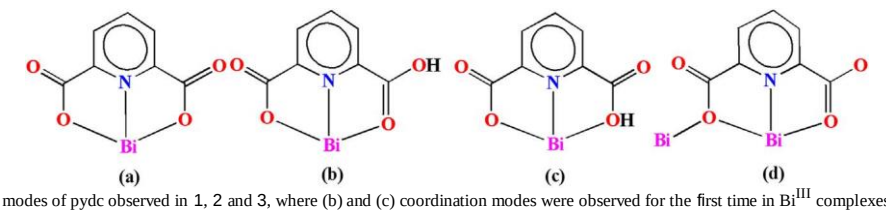

Scheme 1. Different coordination modes of pydc observed in 1, 2 and 3, where (b) and (c) coordination modes were observed for the first time in Bi^{III} complexes with dipicolinate ligand.

2.2. Synthesis of $(2\text{-apyH})_2[Bi(pydc)_2(pydcH)]\cdot 2H_2O$, 1, $(4\text{-apyH})[Bi(pydc)(pydcH)_2]\cdot 4H_2O$, 2 and $(pipzeaH)[Bi_2(pydc)_3(pydcH)(H_2O)_2]\cdot 5H_2O$, 3

Compound 1 and 3 were synthesized by the refluxing of $pydcH_2$ (0.33 mmol, 54 mg) and $Bi(NO_3)_3\$5H_2O$ (0.11 mmol, 53.36 mg) with different organic amines (2-apy ¼ 0.33 mmol, 31 mg; 4-apy ¼ 0.33 mmol, 31 mg and pipzea ¼ 0.33 mmol, 43 mg) in H_2O solution for 6 h. The resulting solution was cooled down to room temperature and X-ray quality single crystals were obtained by slow solvent evaporation. A synthesis procedure is shown in Scheme 2. For 1: yield of approximate 55% based on bismuth. M.p.: decomposed >255 C. Elemental analysis based on the formula $C_{31}H_{28}N_7O_{14}Bi$, 1(%): Calc. C, 39.93; H, 3.01; N, 10.52. Found(%): C, 40.01; H, 2.95; N, 10.39. FTIR (KBr, cm ^{1}):3340(m), 3193(m), 3093(m), 2900(m), 2638(m), 1643(s), 1554 (s), 1527(s), 1434(m), 1380(s), 1272(s), 1195(s), 1072(s), 1018(s), 918(s),833(s), 732(s), 663(w), 516(w). ^{1}H NMR (DMSO) ¼ 8.32 (s, $3H_4$, [pydc]), 8.23 (s, $6H_{3,5}$, [pydc]), 7.95 (m, $2H_6$, [2-apyH^{b}]), 7.86 (m, $2H_4$, [2-apyH^{b}]), 6.93 (m, $2H_5$, [2-apyH^{b}]),6.82 (m, $2H_3$, [2-apyH^{b}]), 3.44 (br, $4H_{Amin}$, [2-apyH^{b}], $2H_{water}$) ppm. UVeVis (aqueous solution) (l, nm): 275. For 2 Yield of approximate 62% based on bismuth. M.p.: decom-posed >260 C; elemental analysis based on the formula $C_{26}H_{26}N_5O_{16}Bi$, 2(%): Calc. C, 37.25; H, 2.98; N, 8.01; Found(%): C, 37.05; H, 2.94; N, 7.96. FTIR (KBr pellet, cm ^{1}): 3340(m), 3155(m), 3050(m), 2910(m), 2692(m.), 1620(m), 1535(s), 1427(m), 1373(w), 1265(m), 1188(s), 1072(s), 1010(m), 902(w), 833(w), 763(s), 709(w), 649(w), 509(w). ^{1}H NMR (DMSO) ¼ 8.32 (s, $3H_4$, [pydc]), 8.21 (s, $6H_{3,5}$, [pydc]), 8.13 (m, $2H_2$, [4-apyH^{b}]), 6.81 (m, $2H_3$, [4-apyH^{b}]), 3.43 (br, $2H_{Amin}$, [4-apyH^{b}], $4H_{water}$) ppm. UVeVis (aqueous solu-tion) (l, nm): 230, 290. For 3 Yield of approximate 52% based on bismuth. M.p.: decomposed >320 C; elemental analysis based on the formula $C_{34}H_{43}N_7O_{23}Bi_2$, 3(%): Calc. C, 30.55; H, 3.22; N, 7.34; Found(%): C, 30.15; H, 3.24; N, 7.28. FTIR (KBr pellet, cm ^{1}): 3432(m), 3159(m), 3077(m), 2816(m), 1621(s), 1607(s), 1581(s), 1565(s), 1429(s), 1374(s), 1280(m), 1080(s), 1005(m), 911(w), 863(w), 780(s), 735(w), 670(w), 584(w),529(w). ^{1}H NMR (DMSO) ¼ 8.48 (m, $4H_4$, [pydc]), 8.31 (s, $8H_{3,5}$, [pydc]), 2.55 (s, $8H_{2,3,5,6}$, $4H_{1,2}$, [pipzeaH^{b}]) ppm. UVeVis (aqueous solution) (l, nm): 270.

3. Results and discussion

3.1. Spectroscopic studies

Infrared spectroscopy data confirm the coordination of pydc ligand to bismuth (III) ion via the carboxylate group in 1e3. The band associated to the antisymmetric stretching vibrational mode, $n_{as}(eCOO^{e})$, appears at 1643 cm ^{1} and 1620 cm ^{1} in 1 and 2, (1699 cm ^{1} in the free ligand [49]), respectively; while the band associated to symmetric stretching vibrational mode, $n_{s}(eCOO^{e})$, appears at 1380 and 1373 cm ^{1} in 1 and 2 (1332 cm ^{1} in the free

Table 1
Crystallographic data for compounds 1, 2 and 3.

	(2-apyH)$_2$[Bi(pydc)$_2$(pydcH)]·2H$_2$O, 1	(4-apyH)[Bi(pydc) (pydcH)$_2$] ·4H$_2$O, 2	(pipzeaH)[Bi$_2$(pydc)$_4$(H$_2$O)$_2$] ·5H$_2$O, 3
Empirical formula	$C_{31}H_{28}N_7O_{14}Bi$	$C_{26}H_{26}N_5O_{16}Bi$	$C_{34}H_{42}N_7O_{23}Bi_2$
Formula weight	931.58	873.50	1334.71
Temperature/K	294(2)	293(2)	293(2)
Wavelength/Å	0.71073	0.71073	0.71073
Crystal system	Triclinic	Triclinic	Monoclinic
Space group	$P\bar{1}$	$P\bar{1}$	$P2_1/c$
Z	2	2	4
Unit cell dimensions	a =11.6659 (5) Å b = 12.0081 (5)Å c = 13.8719 (5)Å α = 94.511 (2) β = 108.139 (2) γ = 111.158 (2)	A = 10.7136(4) Å b=13.0245(5) Å c=16.1537(9) Å α = 107.589(1) β = 104.616(1) γ = 103.575(2)	a=16.3203(4) Å b = 11.9924(3) Å c = 23.1712(6) Å β = 106.757(3)
Absorption coefficient/	5.324 mm^{-1}	6.05 mm^{-1}	8.19 mm^{-1}
Min. and max. transmission factor	0.85e1.00	0.40e1.00	0.28e1.00
F(000)	916	856	2584
Theta range for data collection	1.58 to 35.25	3.23 to 32.68	3.23 to 32.75
Index ranges	18 < h < 18, 19 < k < 19, 21 < l < 22	11 < h < 11, 15 < k < 15, 16 < l < 16	22 < h < 24, 18< k < 16, 34 < l < 34
Reflections collected	71564	19750	14510
Completeness to theta	99.1% (to theta 35.25)	90.6% (to theta 32.75)	90.6% (to theta 35.75)
Refinement method	Full-matrix least-squares on F^2	Full-matrix least-squares on F^2	Full-matrix least-squares on F^2
Data/restraints/parameters	14969/0/495	6041/8/451	14510/0/585
Goodness-of-fit on F^2	1.034	1.045	1.008
Final R indices [I > 2sigma(I)]	R1 = 0.0198, wR2 = 0.0425	R1 = 0.0187, wR2 = 0.0582	R1 = 0.0481, wR2 = 0.0738
R indices (all data)	R1 = 0.0256, wR2 = 0.0438	R1 = 0.0202, wR2 = 0.0642	R1 = 0.0945, wR2 = 0.0869
Largest diff. peak and hole	0.671and 0.764 e.Å^{-3}	0.878 and 0.639e.Å^{-3}	1.20 and 1.02 e.Å^{-3}

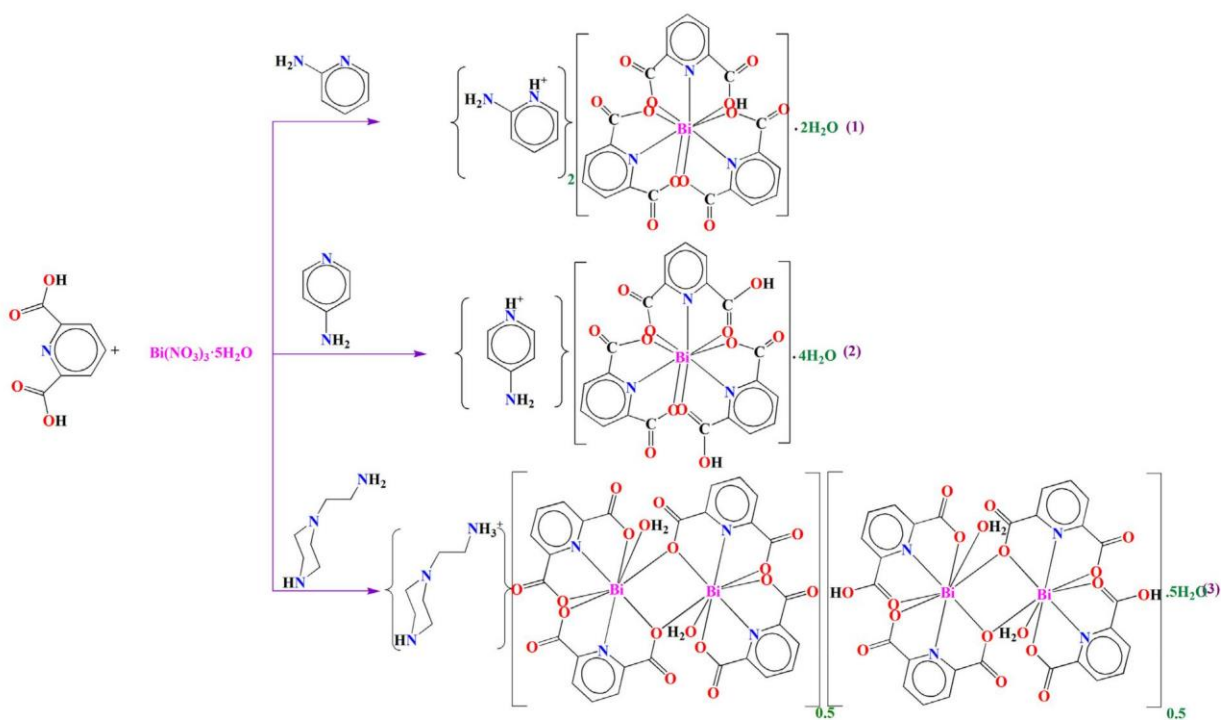

Scheme 2. Preparation route to compounds 1, 2 and 3.

ligand [60]). The value of Δ (ν_{as}(COO$^-$) ν_s(COO$^-$)), amounts to 263 cm^{-1} for 1, and 247 cm^{-1} for 2, indicating the presence of a carboxylate group coordinated to bismuth(III) ion in the unidentate mode [61,62]. The separation for unidentate carboxylate groups is >200 cm^{-1}, whereas it is <200 cm^{-1} in the bidentate ones [61]. Confirming the presence of (NH)$^+$ group, can be achieved from the presence of bands at 3193 cm^{-1} in 1 as well as 3155 cm^{-1} in 2, due to stretching. Broad band in 3093 cm^{-1} for 1 and 3050 cm^{-1} for 2 is due to stretching vibrations of aromatic C–H's of 2-apyH$^+$, 4-apyH$^+$ and pydc ions, respectively. The carboxyl O–H stretching frequency (2900 cm^{-1} in 1 and 2910 cm^{-1} in 2) is also observed. Moreover, the sharp bands in 1554 cm^{-1} and 1434 cm^{-1} in 1 as well as 1535 cm^{-1} and

1427 cm ^{1} in 2 are attributed to aromatic C]C and bands in 1272 cm ^{1} and 1072 cm ^{1} in 1 in addition to 1265 cm ^{1} and 1072 cm ^{1} in 2, are related to various CeN groups. Finally, sharp bands in 918e732 cm ^{1} in 1 and 902e709 cm ^{1} in 2 are due to out-of-plane aromatic C,H.

The IR spectrum of 3 shows a broad band in 3100e3400 cm ^{1} due to n(OH) stretching vibrations of water molecules and pyri-dine-2,6-dicarboxylic acid; the broadness of this band indicates the presence of hydrogen bonds involving water molecules in 3. The broad band in 3077 cm ^{1} is due to stretching vibrations of aromatic CeH's of pydc. Also, the broad and branched peak at 2816e3432 cm ^{1} is attributed to aliphatic CeH's of pipzeaH^{þ} and aromatic CeH's of pydc. Strong peak in 1581 cm ^{1} is attributed to bending vibration of NH$^{þ}_{3}$ group. The sharp and relatively strong band in 1080 cm ^{1}is attributed to CeN stretching vibration. In the region of 1565e1429 cm ^{1}, the sharp and relatively strong peaks found are attributed to the aromatic C]C of pydc ring. Also, some strong peaks in 1621 cm^{1}, together with a strong peak in 1374 cm ^{1}, are due to n_{as}(eCOO) and n_{s}(eCOO), respectively. The value of D (n_{as}(eCOO) n_{s}(eCOO)), amounts to 249 cm ^{1} for 3, indicating the unidentate coordination mode of carboxylate group to bismu-th(III) ion, as the carboxylate group is considered to be bridging only if both carboxylate oxygen atoms are coordinated to two different metal ions [60]. In the case of 3, only one carboxylate oxygen atom is coordinated to bismuth(III) ions, with the other being uncoordinated, which is similar to unidentate coordination mode of carboxylate group. The value of D is in agreement with this assumption [61]. Sharp bands in 911e735 cm ^{1} in 3 are due to out-of-plane aromatic CeH.

In ^{1}H NMR spectra (Scheme S1 and Figs. S1,S3), there are three clear characteristic sets of resonances at 8.21e8.48 ppm for hy-drogens of pydc fragment [10]. The other resonances are attributed to the hydrogens of different amines. The UVeVis spectra of aqueous solution of 1, 2 and 3 show only one band, illustrated in Fig. S4. The absorption with a maximum in the range 200e300 nm can be assigned to intraligand p/p* and n/p* (carboxyl C]O) transitions of pydc group. To study the thermal stability of com-plexes 1e3, thermal gravimetric analysis (TG) was performed in the temperature range of 25e800 C with the heating rate of 10 C/min in a N_2 atmosphere (Fig. S5). For 1, The TG curve shows that this compound exhibits three steps of weight loss. The first stages are related to removal of two molecules of lattice water in the range 95e150 C with a weight loss of 3.78% (theoretical loss 3.86%). The second step between 230 C and 320 C is related to the release of the 2-apy with a weight loss of 20.76% (theoretical loss 20.20%). The third stage between 350 C and 450 C corresponds to the loss of pydc molecules followed by complete destruction of the structure in 800 C. The final mass remnant of 54.03% is indicative of depo-sition of Bi_2O_3, (theoretical residue of Bi_2O_3: 50.02%). For 2, The TG curve shows that this compound exhibits three steps of weight loss. The first stages are related to removal of four molecules of lattice water in the range 80e160 C with a weight loss of 8.72% (theo-retical loss 8.24%). The second step between 260 C and 330 C is related to the release of the 4-apy with a weight loss of 10.89% (theoretical loss 10.77%). The third stage between 340 C and 460 C corresponds to the loss of pydc molecules followed by complete destruction of the structure in 800 C. The final mass remnant of 54.03% is indicative of deposition of Bi_2O_3, (theoretical residue of Bi_2O_3: 53.34%). The TG curve for compound 3 shows that this compound exhibits three steps of weight loss. The first stages in the range 80e280 C are related to removal of crystallization water molecules and coordinated water molecules (found: 9.42%, calcd: 9.44%). The second stage in the range 300e350 C is related to the release of pipzea (found: 8.29%, calcd: 9.68%). The third stage from 350 C to 400 C corresponds to the loss of pydc molecule followed by complete destruction of the structure to 800 C. Nevertheless the final remnants of 45.55% suggests that the complex does not decomposed completely under the experimental temperature (theoretical residue of Bi_2O_3 34.91%).

3.2. X-ray crystallographic structures

The crystallographic data of 1, 2 and 3 are given in Table 1, selected bond lengths and angles are listed in Table 2 and the hydrogen bond geometry in Table 3.

3.2.1. Structures of (2-apyH)$_2$[Bi(pydc)$_2$(pydcH)]·2H$_2$O, 1 and (4-apyH)[Bi(pydc) (pydcH)$_2$]·4H$_2$O, 2

Both compounds 1 and 2 crystallized in a triclinic space group and have monomeric units in which the pydc or pydcH moieties act as tridentate ligands, H-bonded to 2-apy or 4-apy cations. The protonated position in the cationic counter ions of both is the pyridine nitrogen atom. In the anionic complexes of 1 and 2, the Bi(III) is nine-coordinated by three nitrogen atoms and six oxygen atoms of carboxylate from pydc, protonated or deprotonated oxy-gen atom from pydcH fragments. The Bi-O bond lengths are in the range 2.2637(29)e2.8281(27) Å and the BieN bond lengths are in the range 2.4324(15)-2.6665(15) Å (Table 2). The average values of Bi-O and Bi-N bond lengths are comparable with the corresponding ones reported in the literature for related bismuth(III) complexes with pyridine-2,6-dicarboxylate or 4-hydroxy pyridine-2,6-dicarboxylate [12,15e18,35,36,45-51].

Table 2
Selected bond distances and bond angles (Å,) for Compounds 1, 2 and 3.

Compound 1, (2-apyH)$_2$[Bi(pydc)$_2$(pydcH)]·2H$_2$O			
Bi1eO10	2.3216(11)	Bi1eO32	2.3702(10)
Bi1eO12	2.5252(14)	Bi1eN10	2.4324(15)
Bi1eO21	2.4948(13)	Bi1eN20	2.5683(12)
Bi1eO22	2.5297(13)	Bi1eN30	2.6665(15)
Bi1eO30	2.7946(10)		
O10eBi1eO32	77.757(41)	O22eBi1eO30	86.463(39)
O32eBi1eO22	81.603(44)	O10eBi1eO21	86.840(48)
O10eBi1eO22	77.837(45)	O12eBi1eO32	91.889(42)
O21eBi1eO30	84.676(42)	N10eBi1eN30	120.392(43)
O12eBi1eO30	69.400(36)	N20eBi1eN30	112.952(38)
O21eBi1eO12	76.144(48)	N10eBi1eN20	125.281(39)
Compound 2, (4-apyH)[Bi(pydc) (pydcH)$_2$]·4H$_2$O			
Bi1eO4	2.754 (2)	Bi1e O2	2.264(2)
Bi1eO5	2.577 (2)	Bi 1dN1	2.539(2)
Bi1eO7	2.397 (2)	Bi 2dN2	2.497(2)
Bi1eO8	2.366 (2)	Bi 3dN3	2.636(2)
Bi1eO9	2.828(3)		
O7eBi1eO8	73.741(88)	O2eBi1eO5	84.287(85)
O2eBi1eO8	79.644(90)	O7eBi1eO9	87.550(78)

O7eBi1eO2	79.864(90)	O4eBi1eO8	81.837(76)
O4eBi1eO9	78.881(78)	N1eBi1eN3	113.604(75)
O5eBi1eO9	82.396(81)	N2eBi1eN3	116.162(78)
O4eBi1eO5	87.484(79)	N1eBi1eN2	129.990(75)

Compound 3, (pipzeaH)[Bi_2(pydc)$_3$(pydcH) (H_2O)$_2$]·5H_2O

Bi1eO1A	2.376 (3)	Bi1eO3B	2.561 (3)
Bi1eO3A	2.466 (3)	Bi1eO3B^{i}	2.632 (3)
Bi1eN1A	2.439 (4)	Bi1eN1B	2.445 (4)
Bi1eO1B	2.308 (3)	Bi1eO11	2.505 (3)
Bi2eO1C	2.399 (4)	Bi2eO1D	2.626 (3)
Bi2eO3C	2.391 (4)	Bi2eO3D	2.307 (3)
Bi2eN1C	2.425 (4)	Bi2eN1D	2.496 (4)
Bi2eO1D^{ii}	2.564 (3)	Bi2eO21	2.510 (4)

Symmetry codes: (i) x, yþ1, zþ1; (ii) xþ1, y, zþ1.

O1BeBi1eO1A	91.8 (1)	O3DdBi2dO3C	87.7 (1)
O1AdBi1dO3B	75.75 (12)	O1D^{ii}dBi2dO1D	71.45 (12)
O3AdBi1dO3B^{i}	90.21 (11)	O3CeBi2eO1D^{ii}	93.05 (13)
N1AdBi1dN1B	125.08 (13)	N1CeBi2eN1D	129.59 (14)
O1AdBi1dO3A	132.1 (1)	O3CeBi2eO1C	132.9 (1)
O1AdBi1dO11	147.5 (1)	O3CeBi2eO21	151.2 (1)
O3AdBi1dO3B	146.3 (1)	O1CeBi2eO1D	140.5 (1)
N1AdBi1dN1B	125.1 (1)	N1CeBi2eN1D	129.6 (1)

Symmetry codes: (i) x, yþ1, zþ1; (ii) xþ1, y, zþ1

Table 3
Hydrogen bond geometry.

DeH$$$A	DeH	H/A	D/A	< DeH/A
Compound 1, (2-apyH)2[Bi(pydc)2(pydcH)]·2H2O.				
O1eH1A$$$O13^{i}	0.83 (5)	2.04 (5)	2.859 (3)	172 (4)
O1eH1B$$$O13	0.77 (4)	1.99 (4)	2.753 (3)	172 (4)
O2eH2A$$$O33^{ii}	0.86 (3)	2.04 (3)	2.890 (2)	174 (2)
O2eH2B$$$O12^{iii}	0.79 (3)	2.04 (3)	2.8221 (18)	175 (2)
O30eH20A$$$O20^{iv}	0.81 (2)	1.75 (2)	2.5516 (19)	171 (2)
N70eH70$$$O22	0.9100	1.8300	2.730 (2)	169.00
N71eH71A$$$O23	0.8600	1.9900	2.834 (2)	170.00
N71eH71B$$$O20^{v}	0.8800	2.1200	2.926 (2)	153.00
N80eH80$$$O2^{v}	0.8600	1.9400	2.790 (2)	168.00
N81eH81A$$$O1^{ii}	0.8800	1.9800	2.823 (3)	159.00
N81eH81B$$$O11	0.8400	1.9800	2.818 (3)	178.00
C15eH15$$$O32^{ii}	0.9300	2.5000	3.258 (2)	138.00
C34eH34$$$O11^{vi}	0.9300	2.4000	3.119 (2)	134.00
C72eH72$$$O33^{vii}	0.9300	2.4800	3.265 (3)	142.00
C84eH84$$$O31^{viii}	0.9300	2.4800	3.140 (3)	128.00
C85eH85$$$O31^{ix}	0.9300	2.3400	3.224 (3)	158.00
Symmetry codes: (i) x, y, zþ1; (ii) xþ1, yþ1, zþ1; (iii) x, yþ1, z; (iv) x, y, z; (v) xþ1, y, z; (vi) x, y 1, z; (vii) xþ2, yþ1, zþ1; (viii) xþ1, y, z; (ix) xþ1, yþ1, z.				
Compound 2, (4-apyH)[Bi(pydc) (pydcH)2]·4H2O.				
O3eH3$$$O16	1.00 (3)	1.64 (4)	2.568 (5)	153 (4)
O10eH10A$$$O17	1.01 (4)	1.60 (4)	2.577 (4)	162 (4)
O14eH14A$$$O17^{i}	0.85	2.12	2.9059	153
O15eH15A$$$O7	0.95	1.94	2.874 (4)	169
O15eH15B$$$O14	0.91	2.09	2.9722	163
O16eH16A$$$O11^{ii}	0.85	2.24	2.922 (5)	138
O16eH16B$$$O14^{iii}	0.85	1.94	2.7594	162
O17eH17A$$$O13^{iii}	0.81	1.92	2.726 (4)	169
O17eH17B$$$O12^{iv}	0.93	1.83	2.756 (4)	169
N4eH4$$$O8	1.03	2.60	3.162 (5)	114
N4eH4$$$O15	1.03	1.87	2.830 (4)	153
N6eH6A$$$O12^{v}	1.01	2.07	2.961 (4)	146
N6eH6B$$$O1^{vi}	1.01	1.93	2.894 (4)	158
C1eH1$$$O13^{vii}	1.08	2.46	3.409 (4)	145
C2eH2$$$O5^{v}	1.08	2.60	3.552 (4)	146
C19eH19$$$O2^{viii}	1.08	2.54	3.187 (4)	117
C25eH25$$$O8	1.08	2.51	3.128 (5)	115
C28eH28$$$O1^{vi}	1.08	2.41	3.248 (5)	134
C29eH29$$$O5^{ix}	1.08	2.44	3.295 (5)	135
Symmetry codes: (i) xþ1, yþ2, z; (ii) xþ1, yþ1, z; (iii) x 1, y, z; (iv) x, yþ2, zþ1; (v) xþ1, yþ1, zþ1; (vi) xþ2, yþ1, zþ1; (vii) x, y 1, z; (viii) xþ1, yþ2, zþ1; (ix) xþ1, y, z				
Compound 3, (pipzeaH)[Bi2(pydc)3(pydcH) (H2O)2]·5H2O				
O11eH11A$$$N2E^{ii}	0.87	2.24	2.993 (8)	145
O11eH11B$$$O4D^{ii}	0.87	1.82	2.689 (6)	174
N1EdH1EA$$$O2A^{iii}	0.86	2.55	2.830 (6)	100
N1EdH1E$$$O4A^{iv}	0.86	2.54	2.831 (6)	159
N3EdH3N$$$O3A^{ii}	0.89	2.05	2.872 (6)	153
N3EdH3NB$$$O2W^{v}	0.89	2.18	2.995 (6)	152
N3EdH3N$$$O5W^{ii}	0.89	2.37	2.920 (6)	120
N3EdH3N$$$O4C^{ii}	0.89	2.02	2.854 (7)	157
O11eH11A$$$N2E^{ii}	0.87	2.24	2.993 (8)	145
O11eH11B$$$O4D^{ii}	0.87	1.82	2.689 (6)	174
O21eH21A$$$O2B^{vi}	0.85	1.92	2.685 (6)	149
O21eH21B$$$O2W	0.83	1.96	2.789 (6)	174
O2AdH2AA$$$N1E$^{(x)}$	0.84	2.12	2.830 (6)	142
O1WeH1WA$$$O3W^{vii}	0.88	2.55	2.875 (6)	103
O1WeH1WB$$$O3W^{vii}	0.83	2.57	2.875 (6)	103

Table 3 (continued)

DeH$$$A	DeH	H/A	D/A	< DeH/A
O2WeH2WA$$$O4W^{ii}	0.85		2.821 (6)	161

		2.01		
O2WeH2WB$$$O2A[iii]	0.97		2.847 (6)	157
		1.93		
O3WeH3WA$$$O2C[ii]	0.84		2.978 (5)	146
		2.25		
O3WeH3WB$$$O2D[v]	0.96		2.761 (5)	148
		1.90		
O5WeH5WA$$$O1W	0.96		2.784 (6)	141
		1.98		
O5WeH5WB$$$O1C[vi]	0.77		2.936 (4)	165
		2.18		
C3BeH3B$$$O2D[vi]	0.93		3.506 (7)	173
		2.58		
C4BeH4BA$$$O1W[xi]	0.93		3.427 (6)	140
		2.66		
C4DdH4D$$$O2C[ix]	0.93		3.028 (6)	121
		2.45		
C5DdH5D$$$O4B[ii]	0.93		3.379 (6)	168
		2.46		
C1EdH1EC$$$O3A[ii]	0.97		3.245	123
		2.62		
C3EdH3E$$$O4W[ii]	0.97		3.134 (7)	120
		2.54		
C3EdH3E$$$O11[ii]	0.97		3.354 (7)	137
		2.58		
C6EdH6EA$$$O5W[ii]	0.97		3.209 (6)	120
		2.61		

Symmetry codes: (ii) xþ1, yþ1, zþ1; (iii) xþ1, y, z; (iv) xþ1, y 1/2, z 1/2; (v) x, yþ1, z; (vi) xþ1, y, zþ1; (vii) xþ1, y 1/2, zþ1/2; (ix) x, y 1/2, z 3/2; (x) x 1, y, z; (xi) x, yþ1/2, zþ1/2.

The three oxygen atoms (O30, O12 and O21 in 1 as well asO7, O8 and O2 in 2) form a triangle and the other three (O10, O22 and O32 in 1, also O4, O5 and O9 in 2) form another triangle. Considering the angles between the oxygen atoms in both 1 and 2, it is found that they are almost eclipsed. So a prism consisted of six oxygen atoms with three caps of nitrogen atoms on its faces are proposed for both.

3.2.1.1. $(2\text{-apyH})_2[Bi(pydc)_2(pydcH)]\cdot 2H_2O$, 1. Compound 1, has an asymmetric unit with one $Bi^{3þ}$ cation, two pydc dianions, one pydcH anion, two 2-apyH cations and also two water molecules

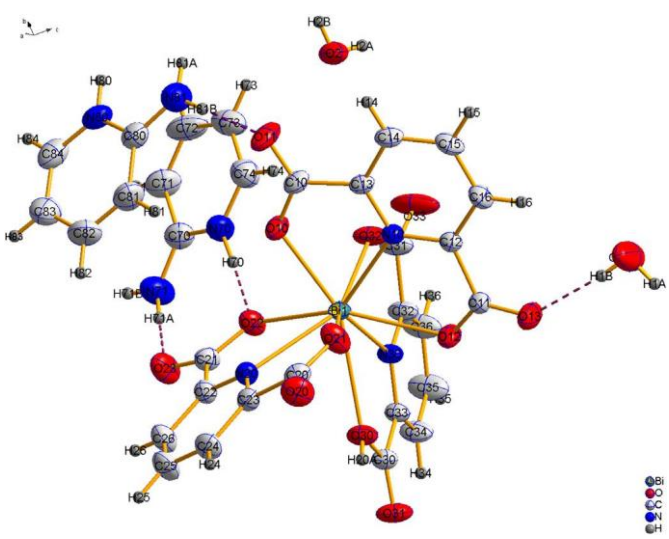

Fig. 1. The molecular and crystal structure of $(2\text{-apyH})_2[Bi(pydc)_2(pydcH)]$\$$2H_2O$, 1, showing the atom-numbering scheme and displacement. Ellipsoids are at the 50% probability level. Hydrogen bonds are shown with dashed lines.

(Fig. 1). The $Bi^{3þ}$ cation is nine-coordinated by six oxygen atoms and three nitrogen atoms from two pydc and one pydcH anions (Fig. S6). The BiN3O6 polyhedron is holodirected with a stereo-chemically inactive lone pair of electrons (Fig. S7). The BieO bond lengths are in the range 2.3216(11)e2.7946(10) Å and the BieN bond lengths are in the range 2.4324(15)e2.6665(15) Å. The bond distance of BieO30$_{protonated\ oxygen}$ is significantly longer (2.7946(10) Å) than the BieO$_{deprotonated\ oxygen}$ bonds (2.3216(11)e2.5297(13) Å). However, it is shorter than the maximum of 3.429 reported for BieO retrieved from the Cambridge Structural Database (CSD) [63]. All two pydc and one pydcH anions exhibit similar coordination modes (Fig. S6) and each coordinates only to one $Bi^{3þ}$ cation.

The carboxylate groups and the pyridyl nitrogen in two pydc and one pydcH anions chelate in a tridentate manner with the same $Bi^{3þ}$ cation to form a $[Bi(pydc)_2(pydcH)]^{2}$ anionic coordination complex with six uncoordinated carboxylate or carboxylic acid oxygens (two from each pydc or pydcH anion). The cation coordi-nation can be rationalized in terms of bond valence [64e66], which assumes that the total charge of the cations has to be saturated by the summation of the separated bond valence s_i of each coordi-nated atom or ion. The quantity s_i can be calculated by the expression s_i ¼ exp[(r_0 r_i)/B], where r_i is the actual BieO or BieN distance, r_0 and B are parameters empirically determined (r_0¼2.094 for BieO, r_0 ¼ 2.02 for BieN, B¼0.37 for BieO and B¼0.35 for BieN). In the present structure, the value of 2.8 for s ¼ s_i obtained for the bismuth cation (Table 4), is in good agreement with the expected charge value of 3.00.

Each anionic monomer interacts non-covalently with three 2-

Table 4
Bond Valence Sum (BVS) for Bi atoms in Compounds 1, 2 and 3.

Bond typ	ri	r0	B	r0-ri/B	B.V
Compound 1, $(2\text{-apyH})_2[Bi(pydc)_2(pydcH)]\cdot 2H_2O$					
BieO12	2.525	2.094	0.37	1.1648	0.31198
BieN10	2.432	2.02	0.35	1.177	0.30820
BieO10	2.323	2.094	0.37	0.6189	0.538
BieO21	2.495	2.094	0.37	1.083	0.3385
BieN20	2.567	2.02	0.35	1.565	0.2090
BieO22	2.530	2.094	0.37	1.178	0.3079
BieO30	2.795	2.094	0.37	1.8945	0.150
BieN30	2.666	2.02	0.35	1.845	0.158
BieO32	2.370	2.094	0.37	0.746	0.474
Compound 2, $(4\text{-apyH})[Bi(pydc)\ (pydcH)_2]\cdot 4H_2O$					
Bi1e O4	2.754 (2)	2.094	0.37	1.7838	0.1680
Bi1e O5	2.577 (2)	2.094	0.37	1.3054	0.2711
Bi1eO7	2.397 (2)	2.094	0.37	0.8189	0.4409
Bi1eO8	2.366 (2)	2.094	0.37	0.7351	0.4794
Bi1eO9	2.828(3)	2.094	0.37	1.9838	0.1375
Bi1e O2	2.264 (2)	2.094	0.37	0.4595	0.6316
Bi 1dN1	2.539 (2)	2.02	0.35	1.4829	0.2270
Bi 2dN2	2.497 (2)	2.02	0.35	1.363	0.2559
Bi 3dN3	2.636 (2)	2.02	0.35	1.760	0.1720
Compound 3, $(pipzeaH)[Bi_2(pydc)_3(pydcH)\ (H_2O)_2]\cdot 5H_2O$					
Bi1eO1B	2.308 (3)	2.094	0.37	0.5784	0.5608
Bi1eO1A	2.376 (3)	2.094	0.37	0.7622	0.4667
Bi1eO3A	2.467 (3)	2.094	0.37	1.0081	0.3649
Bi1eO11	2.504 (3)	2.094	0.37	1.1081	0.3302
Bi1eO3B i	2.561 (3)	2.094	0.37	1.2622	0.2830
Bi1eO3B	2.631 (3)	2.094	0.37	1.4513	0.2342
Bi1eN1A	2.440 (4)	2.02	0.35	1.2	0.3012
Bi1eN1B	2.446 (4)	2.02	0.35	1.2171	0.2961
Bi2eO3D	2.308 (3)	2.094	0.37	0.5784	0.5608
Bi2eO3C	2.391 (4)	2.094	0.37	0.5784	0.5608
Bi2eO1C	2.398 (4)	2.094	0.37	0.8216	0.4397
Bi2eO21 ii	2.508 (4)	2.094	0.37	1.1189	0.3266
Bi2eO1D	2.564 (3)	2.094	0.37	1.2703	0.2807
Bi2eO1D	2.626 (3)	2.094	0.37	1.4378	0.2374
Bi2eN1C	2.424 (4)	2.02	0.35	1.1543	0.3153
Bi2eN1D	2.497 (4)	2.02	0.35	1.3628	0.2559

apyH cations through carboxylate-2-apyH H-bonding. Each coor-dination bismuth unit is connected to two other such units through the 2-apyH cations by H-bonding, leading to the forma-tion of an infinite three-dimensional H-bonded layer structure. As shown in Fig. 2, the carboxyl groups of the pydc and pydcH ligands and water molecules are involved in intermolecular OeH$$$O hydrogen bonding, and form three types of robust hydrogen bond synthons, namely, $R^2_2(8)$ I, $R^2_2(12)$ II and $R^2_2(16)$ III. The other set of hydrogen bonding patterns included NeH/O and CeH/O, are held between the $(2\text{-apyH})^{þ}$, its counter anion and water mole-cules (Table 3). An outstanding feature of compound 1 is the presence of CeH/p stacking interactions. The CeH$$$p distance (measured to the centre of the ring) is 2.990 Å (1 x, y, z) and CeH/p angle is 153.42 (Fig. 3). Other intermolecular interactions that can be observed in the structure of compound 1 are pep stackings between aromatic rings, the strongest one is between N70/C70eC74 and N80/C80eC84 rings with the distance of 3.5847(12) Å between the correspondent centers of gravity (Cg), as shown in Fig. 3. The stacking interactions of the carbonyl groups with the ligands are of importance in the structure of 1 explaining the short intermolecular contacts between O(23)/C(21), 3.160 Å, C(21)/C(21), 3.552 Å (Fig. 3). The spaces between two layers of $[Bi(pydc)_2(pydcH)]^{2e}$ fragments are filled with layers of $(2\text{-apyH})^{þ}$ cations and uncoordinated water molecules. The crystal lattice is aggregated through the concert of intermolecular in-teractions, such as electrostatic attraction between ion pairs, stacking interactions of the carbonyl groups, different kinds of hydrogen bonding (NeH/O, OeH/O and CeH/O), pep and CeH/p stacking interactions.

3.2.1.2. $(4\text{-apyH})[Bi(pydc)(pydcH)_2]\cdot 4H_2O$, 2. Compound 2, has an asymmetric unit with one $Bi^{3þ}$ cation, one pydc dianions, two pydcH anion, one 4-apyH cation and also four water molecules (Fig. 4). The $Bi^{3þ}$ cation is nine-coordinated by six oxygen atoms and three nitrogen atoms from one pydc and two pydcH anions (as in Fig. S8). Similar to 1 the BiN3O6 polyhedron is holodirected with a stereochemically inactive lone pair of electrons. The BieO bond lengths are in the range 2.264(2)e2.828(3) Å and the BieN bond lengths are in the range 2.497(2)e2.636(2) Å. The bond distances of $BieO4_{protonated\ acid}$ (2.754(2) Å) and $BieO9_{protonated\ acid}$ (2.828(3)Å) are slightly longer than the $BieO_{deprotonated\ oxygen}$ bonds (2.264(2)e 2.577(2) Å). All one pydc and two pydcH anions exhibit similar

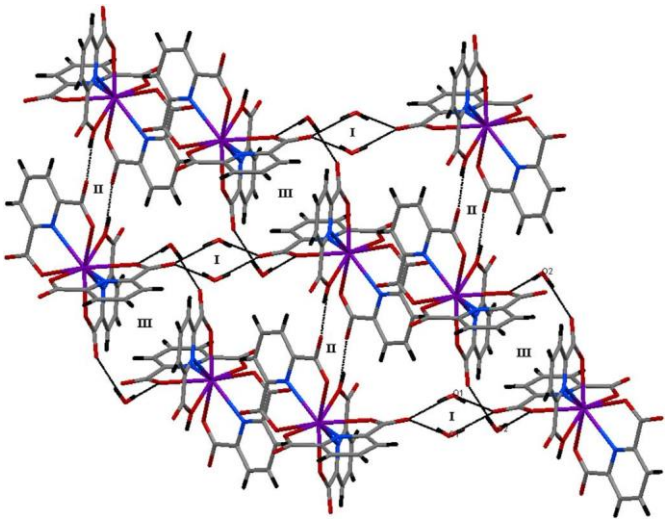

Fig. 2. Graph set descriptors made by OeH$$$O interactions between water ion and $[Bi(pydc)_2(pydcH)]^2$.

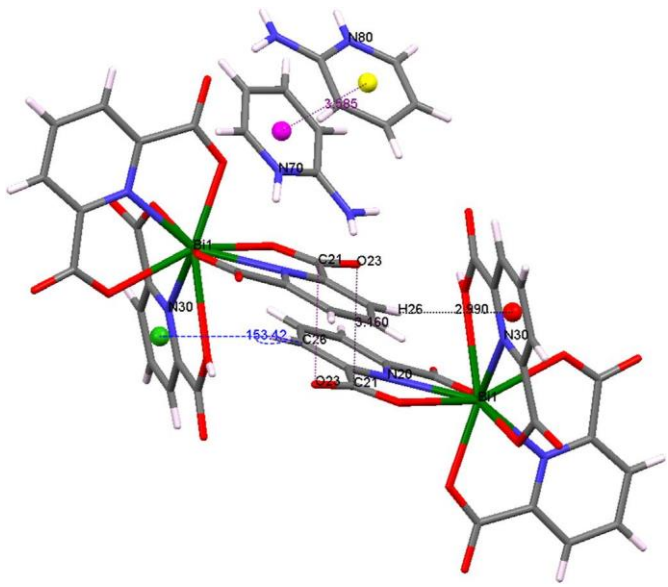

Fig. 3. pep, CeH/p and carbonyl groups stacking interactions in compound 1, The pep stacking between N70/C70eC74 and N80/C80eC84 (x, y, z) rings with the dis-tance of 3.5847(12) Å, The CeH/p distances is 2.990 Å (1 x, y, z) and corresponding CeH/p angle is 153.42 .

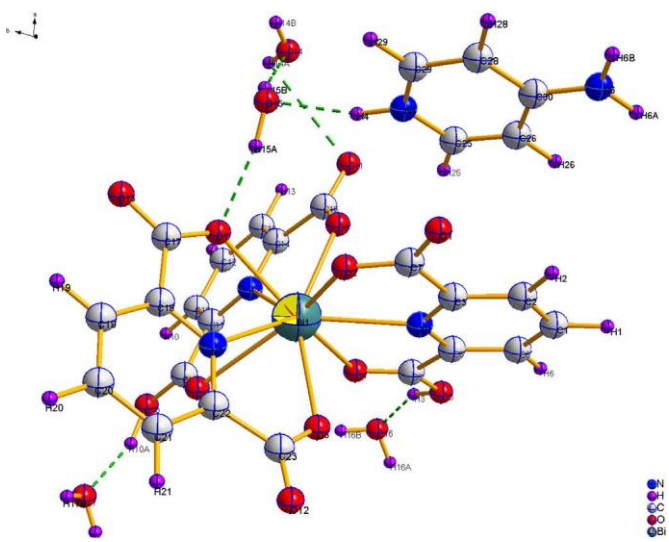

Fig. 4. The molecular and crystal structure of (4-apyH)[Bi(pydc) (pydcH)2]$4H2O, 2, showing the atom-numbering scheme and displacement. Hydrogen bonds are shown with dashed lines.

coordination modes (Fig. 5b) and each coordinates to only one $Bi^{3þ}$ cation, as in 1. In the structure of 2, the value of 2.78 for s_i obtained for the bismuth cation is also in good agreement with the expected charge value of 3.00 (Table 4).

Each anionic monomer interacts non-covalently with three 4-apyH^{þ} cations through carboxylate e4-apyH H bonding. The crys-tal lattice is aggregated through by intermolecular interactions, such as electrostatic attraction between ion pairs, different kinds of hydrogen bonding (OeH/O, NeH/O, CeH/O) and CeO$$$p stacking interactions.

In the crystal structure of 2 the fact that all the components are connected through OeH/O, NeH/O and CeH/O hydrogen bonds, results in an interesting 3D sheet structure. OeH/O hydrogen bonding between the water molecules (O14, O15, O16

and O17) and O atoms of pydc or pydcH form a cyclic graph set that can be described as $R^3_3(10)$ I, $R^{10}_6(20)$ II, $R^6_4(12)$ III; also, the water molecular cluster with n ¼ 4 in the crystal structure of 2 consist of a triangle shape formed by three water molecules in which the last water molecule is in the center (Fig. 5a). A base chain, including water molecules, with O$$$O distances in the range 2.759e2.9722 Å is present between the anionic complexes. The other set of hydrogen bonding patterns, including NeH$$$O and CeH$$$O, are held between the water molecules, $(4\text{-apyH})^{b}$ and its counter anion (Fig. 5b and c). Repetition of weaker CeH$$$O interactions create the hydrogen bonded layer A shown in Fig. 5c.

Each N(4) nitrogen atom of $(4\text{-apyH})^{b}$ is linked as a bifurcated donor to $[Bi(pydc)(pydcH)_2]^-$ unit and water fragment via hydrogen bonding interactions (Table 3 and Fig. 5b). Considering the DdH/A distance 2.830 (4) Å for (N4eH4$$$O15), these intra-molecular interactions are certainly significant. Also the hydrogen bond donor atom in N6eH6A$$$O12(v) [(v): xþ1, yþ1, zþ1] and N6eH6A$$$O1(vi) [(vi): xþ2, yþ1, zþ1] is the coordinated N(6), so the donor bridged hydrogen bond occurs.

Other intermolecular interactions that can be observed in the structure of compound 2 are CeO/p stackings, the strongest one is between C7eO1 and N4/C25eC29 (x,y,z) ring with the distance of 3.167(3) Å (measured to the Cg of the ring), shown in Fig. 6.

3.2.2. $(pipzeaH)[Bi_2(pydc)_3(pydcH)(H_2O)_2]\cdot 5H_2O$, 3

The dimeric bismuth pyridine-2,6-dicarboxylate, 3, has an asymmetric unit of 66 non-hydrogen atoms with two $Bi^{3þ}$ cations, three pydc anions and one pydcH anion, one pipzeaH cation, two terminal water molecules (one for each bismuth ion) and 5 free water molecules (Fig. 7a). Applying the inversion center on the asymmetric unit, the molecular structure of the compound is evi-denced (Fig. 7b): one dimeric neutral $[Bi_2(pydc)_2(pydcH)_2]$ complex and one dimeric anionic $[Bi_2(pydc)_4]^2$ complex are formed (Fig. S9), which represents the most common bridging motif in structurally characterized Bi^{III} complexes with dipicolinate ligands [16,36,46,47,51]. Although there are two distinct bismuth atoms in the asymmetric unit of 3, both $Bi^{3þ}$ cations are eightfold coordi-nated by five oxygen atoms from three different pydc anions, one oxygen from a terminal water molecule, and two nitrogen atoms from two different pydc anions; all the pydc anions chelate in a tridentate manner with the $Bi^{3þ}$ cations involving not only the carboxylate oxygens but also the pyridyl nitrogens (BieN 2.451(4) Å av.).

Unlike compound 1 and 2, the bismuth cation in compound 3 is located in a slightly distorted bicapped octahedral coordination environment, BiN2O6, in which a small effect of the lone pair on the structure asymmetry is observed (Fig. 7c). For each dimer, two of the four pydc fragments bridge the two bismuth ions, each with one oxygen (O3B and O1D). The bridges are asymmetrical

(Bi1eO3B ¼ 2.561(3) Å, Bi1eO3B^{i} ¼ 2.632(3)$_{ii}$Å (i: x, yþ1, zþ1),
Bi2eO1D ¼ 2.626(3) Å, Bi2eO1D ¼ 2.564(3) Å
(ii: xþ1, y, zþ1)) (Fig. S9) and all the bridging BieO distances are longer with respect to the not-bridging BieO bonds (2.375 (4) Å av.). The main difference between the two dimeric molecules is the presence of two hydrogen atoms connected to two oxygens of the non-bridging pydc fragments in one of them i.e. Bi1, and conse-quently the corresponding C1AeO2A distance (1.253 (6) Å) results slightly elongated with respect to the analogue in the other pydc fragments (C]O 1.232 Å av.). The pydc anions exhibit (02110), (01111) and (01110) modes (Fig. S10) [67]. This dimeric compound lies about an inversion centre. The distances between the two bismuth atoms in each dimer are too large for considering a bonding interaction (Bi1eBi1A 4.299(1) Å, Bi2eBi2A 4.214(1) Å) and they agree to similar dimeric complexes (BieBi 4.320 Å) [16]. In the structure of 3, the values of 2.84 and 2.98 for s_i obtained for

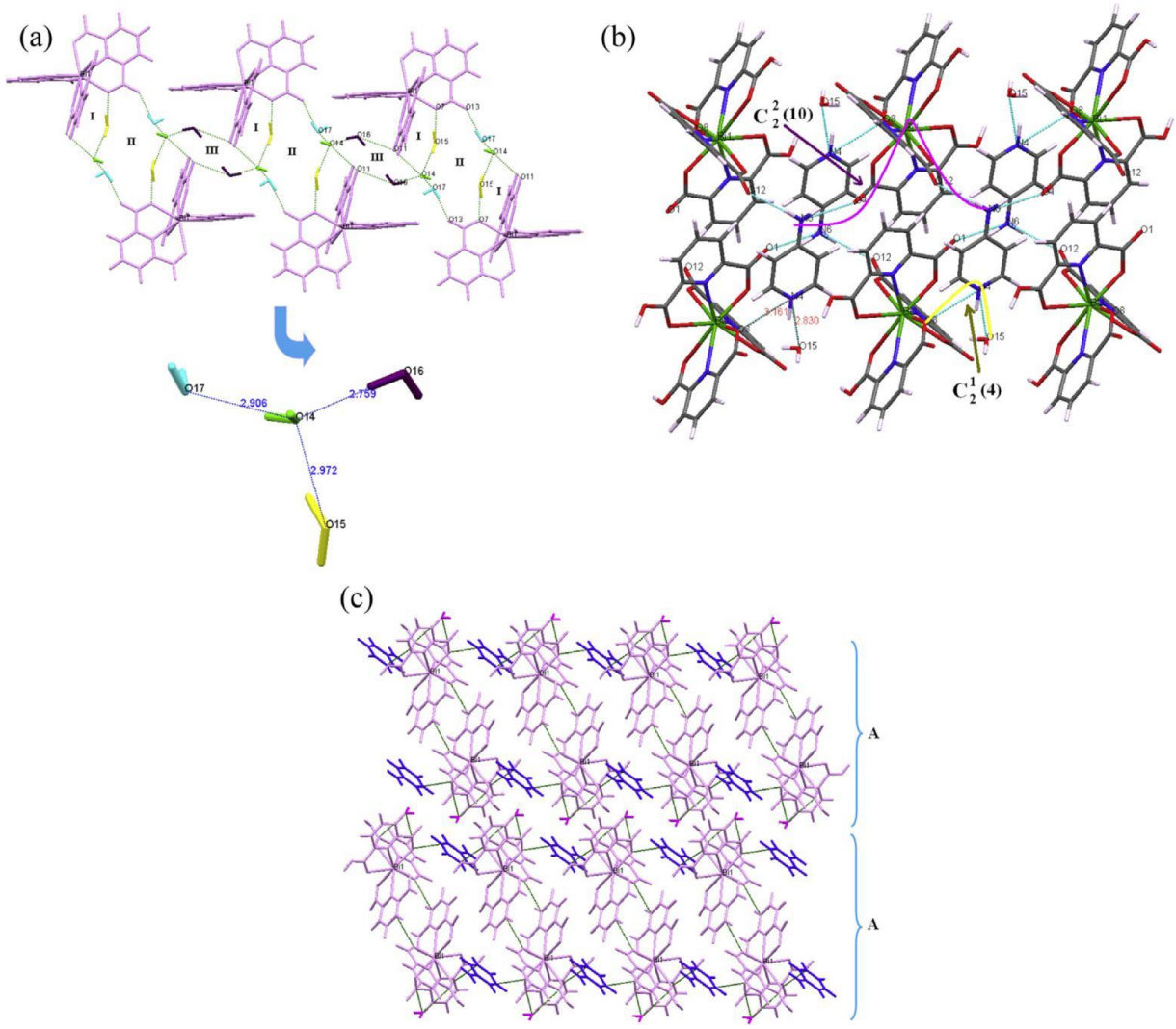

Fig. 5. (a) Graph set descriptors made by OeH/O interactions between water molecules and $[Bi(pydc)_2(pydcH)]^2$ with a view of the triangle shape tetrameric water cluster in 2, (b) A view of 1D chain constructed by NeH/O hydrogen bonds between anionic complexes, cationic fragments and uncoordinated water molecules in 2, (c) Hydrogen bonded layer A made by CeH/O interactions in 2.

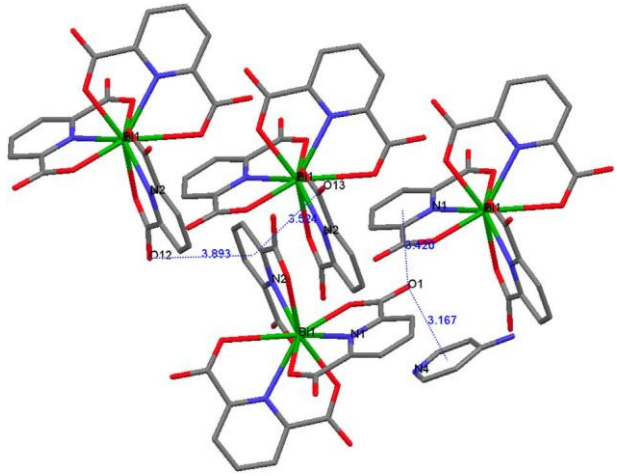

Fig. 6. CeO/p stackings interactions in compound 2, between C7eO1 and N4/ C25eC29 (x, y, z) ring, C7eO1 and N1/C1eC5 (1 x,1 y,1 z) ring, C23eO12 and N2/ C18eC22 (x,2 y,1 z) ring and C17eO13 and N2/C18eC22 (1 x,2 y,1 z) ring with the distances of 3.167(3), 3.420(3), 3.893(3) and 3.524(3)Å, respectively.

the Bi1 and Bi2 cations, respectively, are also in good agreement with the expected charge value of 3.00 (Table 4).

There are extensive intermolecular OeH$$$O, NeH$$$O and weak CeH$$$O hydrogen bonds, which cause the stability of the crystal structure (Table 3). The dimeric neutral and anionic molecules are disposed through alternate rows in the [010] di-rection, leading to the formation of an infinite three-dimensional H-bonded layer structure parallel to the (001) plane, in which all the molecules are directly connected by two strong (O21eH21A/O2B 2.685(6) Å and O11eH11B/O4D 2.689(6) Å) and two weaker (C5DeH5D/O4B 2.463 Å and C3BeH3B/O2D 2.581 Å) hydrogen bonds and also some pep stacking in-teractions between the pydc rings along the neutral molecules rows N1A/C2AeC6A rings with the distance of 3.903(3) Å (cen-troidecentroid distances) (Fig. 8a and b). The molecules of different planes are connected each other by the short hydrogen bond C4DeH4D/O2C (3.028(8) Å). Thus the molecules of the complex are directly interconnected in all directions of the crystal, without involving the pipzeaH cation and the free water molecules. The volume between the (001) planes is filled by the pipzeaH cations, connected to the dimeric molecules through

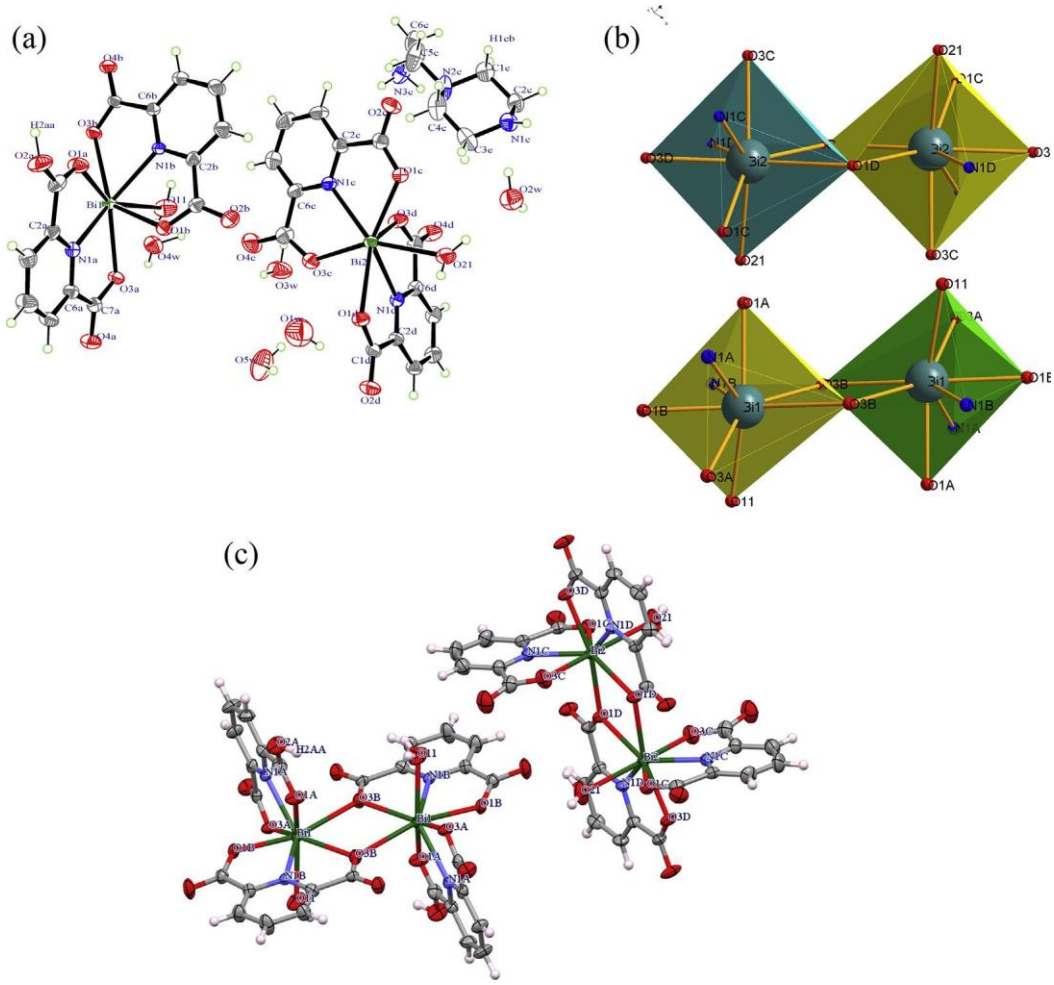

Fig. 7. (a) Asymmetric unit content of (pipzeaH)[Bi_2(pydc)$_3$(pydcH) (H_2O)$_2$].5H_2O, 3, showing the atom-labeling. Ellipsoids are at the 40% probability level; (b) Polyhedron showing the bicapped octahedral coordination environment, BiN2O6, at bismuth centers in 3; (c)Various coordination modes exhibited by pydc and pydcH anions in compound 3.

NeH/O, OeH$$$N and CeH/O bonding.

Noteworthy is the strong hydrogen bond that involves the hydrogen connected to the oxygen of one pydc fragment and the positi ve charged N1E of the pipzeaH cation (O2AeH2AA/N1E 2.822(7) Å) (Fig. 8b). Clearly the acid H2AA is strongly attracted from the positive charge of the N1E atom, and this is the reason for the possibility to easily localize this hydrogen with X-ray diffrac-tion; the consequence of this strong interaction is that the hydrogen connected to the N1E is very near to H2AA (H1EA/H2AA ¼ 1.61 Å) and thus in this case the hydrogen repul-sion is negligible with respect to the electrostatic force connecting H2AA with N1E.

Finally, between the (001) planes are disposed also the free water molecules that contribute to the stabilization of the crystal packing, bonding both the pydc, the coordinated water ligands and the pipzeaH cations, through a great number of strong and weak hydrogen bonds (Table 3). As shown in Fig. 8c, the water molecules are involved in intermolecular OeH/O hydrogen bonding, and form a one-branched chain of the water molecules with the for-mula of (H_2O)$_6$.

4. Conclusion

Three new metal-organic compounds containing bismuth and pyridine-2,6-dicarboxylate (pydc), (2-apyH)$_2$[Bi(pydc)$_2$(pydcH)]$ 2H_2O, 1, (4-apyH)[Bi(pydc)(pydcH)$_2$]4H_2O$, 2 and (pipzeaH) [$Bi_2$(pydc) $_3$(pydcH) (H_2O)$_2$]5H_2O$, 3 (pydc ¼ pyridine-2,6-dicarboxylate, 2-apy ¼ 2-aminopyridine, 4-apy ¼ 4-aminopyridine, pipzea ¼ 2-piperazin-1-ylethanamine), with zero-dimensional structures have been synthesized via proton transfer methodology and structurally characterized. The proton transfer methodology is utilized as a useful method for the preparation of anionic complexes. Variation in the coordination and H-bonded structure is achieved by varying the amines in the synthesis. Compounds 1 and 2 display similar bismuth coordination envi-ronments with a stereochemically inactive lone pair of bismuth. Also four different coordination modes of metal-dipicolinate exist in 1, 2 and 3. Comparison of our results in the solid state confirms the theory that complexation behavior of bismuth dipicolinate in the same synthetic conditions depends on using different organic amines as counter cation precursors leading to different structural entities. Furthermore, four different coordination modes of metal-dipicolinate exist in 1, 2 and 3, of which two are rare coordina-tion types; one involving metal coordination to the short C]O(BiO) bond of the protonated acid, which is quite rare in the bismuth

dipicolinate complexes; the other which involves metal coordina-tion to a protonated oxygen atom; that has not yet been reported in the bismuth dipicolinate complexes. Fascinating crystal packing

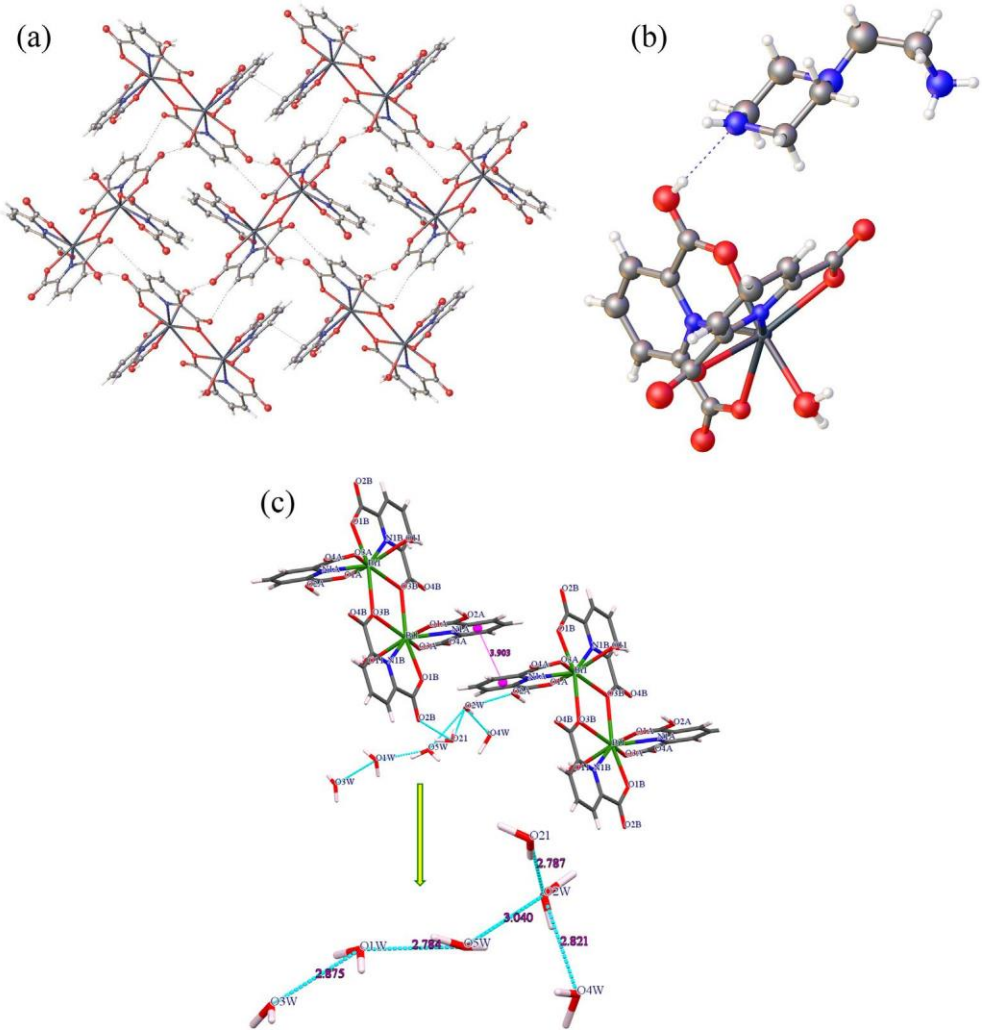

Fig. 8. (a) View of the (001) plane of the crystal packing of 3. Hydrogen bonds and aromatic stacking pep interactions are shown with dashed lines; (b) the strong hydrogen bond that involves the hydrogen connected to the oxygen of one pydc fragment and the positive charged N1E of the pipzeaH cation in 3; (c) pep stacking interactions and a view of the hexameric water cluster in 3, the pep stacking between N1a/C2a-C6a (x, y,1 z) rings with the distance of 3.903(3) Å.

motif results from the concert of intermolecular interactions, such as electrostatic attraction between ion pairs, different kinds of hydrogen bonding (OeH/O, NeH/O, CeH/O) and stacking interactions.

Acknowledgment

This work was supported from funds from FEDER (Programa Operacional Factores de Competitividade COMPETE) and from FCT e Fundaçao~ para a Ciencia^ e Tecnologia under the project Pest-C/ FIC/UI0036/2011 and from Italian MIUR (CONFIN08). The authors are grateful for the crystallography services Coimbra (CEMDRX).

Supplementary data

Crystallographic data for the three structures have been deposited with the Cambridge Crystallographic Data Centre, CCDC 874050 for compound 1, CCDC 874056 for compound 2 and CCDC 918173 for compound 3. Copies of the data can be obtained free of charge on application to the Director, CCDC, 12 Union Road, Cam-bridge CB2 1EZ, UK (Fax. þ44 1223 336033; e-mail: deposit@ccdc. cam.ac.uk or www: http://www.ccdc.cam.ac.uk). Plots of NMR,

UV and TGA spectra together with additional figures are also available in supplementary data.

Appendix A. Supplementary data

Supplementary data related to this article can be found at http:// dx.doi.org/10.1016/j.molstruc.2015.06.084.

References

[1] J. Della Rocca, D. Liu, W. Lin, Acc. Chem. Res. 44 (2011) 957e968.
[2] X.J. Zhang, M.A. Ballem, Z.J. Hu, P. Bergman, K. Uvdal, Angew. Chem. Int. Ed. 50 (25) (2011) 5729e5733.
[3] J.C. Tan, A.K. Cheetham, Chem. Soc. Rev. 40 (2011) 1059e1080.
[4] M. Hakimi, Z. Mardani, K. Moeini, M.A. Fernandes, J. Coord. Chem. 65 (13) (2012) 2221e2233.
[5] M. Hakimi, M. Maeder, G.A. Lawrance, J. Coord. Chem. 64 (1) (2011) 105e114.
[6] M. Hakimi, Z. Mardani, K. Moeini, M. Minoura, H. Raissi, Z. Naturforsch., B: Chem. Sci. 66b (11) (2011) 1122e1126.
[7] M. Hakimi, H. Vahedi, M. Rezvaninezhad, E. Schuh, F. Mohr, J. Sulfur Chem. 32 (1) (2011) 55e61.
[8] M. Hakimi, B.-M. Kukovec, M. Rezvaninezhad, E. Schuh, F. Mohr, Z. Anorg. Allg. Chem. 637 (2011) 1e7.
[9] M. Hakimi, E. Motieiyan, A. Shokrollahi, A. Naghashian Haghighi, Inorg. Chim. Acta 385 (2012) 140e149.
[10] H. Aghabozorg, E. Motieiyan, A.R. Salimi, M. Mirzaei, A. Shokrollahi, S. Derki,

M. Ghadermazi, Sh Sheshmani, H. Eshtiagh-Hosseini, Polyhedron 29 (2010) 1453e1464.

[11] C.N.R. Rao, S. Natarajan, R. Vaidhyanathan, Angew. Chem. Int. Ed. 43 (2004) 1466e1496.
[12] K.P. Rao, A. Thirumurugan, C.N.R. Rao, Chem.ur. J. 13 (2007) 3193e3201.
[13] M. Hakimi, B.-M. Kukovec, M. Minoura, J. Chem. Crystallogr. 42 (2012) 290e294.

[14] M. Hakimi, B.-M. Kukovec, E. Schuh, Z. Noormohammadzadeh, F. Mohr, J. Chem. Crystallogr. 42 (2012) 180e185.
[15] D. Banerjee, S.J. Kim, J.B. Parise, Cryst. Growth Des. 9 (2009) 2500e2503.
[16] A. Thirumurugan, W. Li, A.K. Cheetham, Dalton Trans. 41 (2012) 4126e4134.
[17] O. Anjaneyulu, T.K. Prasad, K.C.K. Swamy, Dalton Trans. 39 (2010) 1935e1940.
[18] A. Thirumurugan, A.K. Cheetham, Eur. J. Inorg. Chem. (2010) 3823e3828.
[19] T. Douki, B. Setlow, P. Setlow, J. Photochem. Photobio. B4 (2005) 591e597.
[20] Y. Kazuhiro, Y. Noriko, F. Tadayasu, Eur. Patent EP0603165, (1994).
[21] G.A. Burdock, Encyclopedia of Food and Color Additives, vol. 3, CRC Press, 1996.

[22] H. Park, A.J. Lough, J.C. Kim, M.H. Jeong, Y.S. Kang, Inorg. Chim. Acta 360 (2007) 2819e2823.
[23] V.H. Rodrigues, M. Hakimi, E. Motieiyan, Acta Crystallogr. E68 (2012) O1524.
[24] S.K. Seth, I. Saha, C. Estarellas, A. Frontera, T. Kar, S. Mukhopadhyay, Cryst. Growth Des. 11 (2011) 3250e3265.
[25] B. Sarma, N.K. Nath, B.R. Bhogala, A. Nangia, Cryst. Growth Des. 9 (3) (2009) 1546e1557.
[26] H. Aghabozorg, Sh Daneshvar, E. Motyeian, F. Manteghi, R. Khadivi, M. Ghadermazi, A. Shokrollahi, M. Ghaedi, S. Derki, M. Shamsipur, J. Iran. Chem. Soc. 6 (3) (2009) 620e637.
[27] C. Yuste, M.R. Silva, M. Ghadermazi, F. Feiz, E. Motieiyan, Acta Crystallogr. E66 (2010) m1643em1644.
[28] J. Safaei-Ghomi, E. Motieiyan, F. Manteghi, M. Ghadermazi, H. Aghabozorg, Acta Crystallogr. E66 (2010) m1016em1017.
[29] C. Yenikaya, N. Büyükkidan, M. Sari, H. Ilkimen, M. Bülbül, O. Büyükgüngor,€ J. Coord. Chem. 64 (2011) 3353e3365.
[30] J.R.H. Xie, V.H. Smith Jr., R.E. Allen, Chem. Phys. 322 (2006) 254e262.
[31] J.T. Groves, I.O. Kady, Inorg. Chem. 32 (1993) 3868e3872.
[32] B.R. Cameron, M.C. Darkes, I.R. Baird, R.T. Skerlj, Z.L. Santucci, S.P. Fricker, Inorg. Chem. 42 (2003) 4102e4108.
[33] A.C. Wibowo, M.D. Smith, H.-C. zur Loye, Cryst. Eng. Comm. 13 (2011) 426e429.

[34] A.C. Wibowo, S.A. Vaughn, M.D. Smith, H.-C. zur Loye, Inorg. Chem. 49 (2010) 11001e11008.
[35] O. Anjaneyulu, K.C.K. Swamy, J. Chem. Sci. 123 (2) (2011) 131e137.
[36] V. Stavila, R.L. Davidovich, A. Gulea, K.H. Whitmire, Coord. Chem. Rev. 250 (2006) 2782e2810.
[37] R. Ge, H. Sun, Acc. Chem. Res. 40 (2007) 267e274.
[38] P. Malfertheiner, Nat. Rev. Gastroenterol. Hepatol. 7 (2010) 538e539.
[39] V. Andre, A. Hardeman, I. Halasz, R.S. Stein, G.J. Jackson, D.G. Reid, M.J. Duer, C. Curfs, M.T. Duarte, T. Friscic, Angew. Chem. Int. Ed. Engl. 50 (2011) 7858e7861.

[40] PhC. Andrews, V.L. Blair, R.L. Ferrero, P.C. Junk, I. Kumar, Chem. Commun. 49

(2013) 2870e2872.
[41] W. Li, L. Jin, N.Y. Zhu, X.M. Hou, F. Deng, H. Sun, J. Am. Chem. Soc. 125 (2003) 12408e12409.
[42] X.-P. Zhang, H.-R. Tian, G.-F. Yan, Y. Su, Y.-L. Feng, J.-W. Cheng, Dalton Trans. 42 (2013) 1088e1093.
[43] M. Feyand, E. Mugnaioli, F. Vermoortele, B. Bueken, J.M. Dieterich, T. Reimer, U. Kolb, D. Vos, N. Stock, Angew. Chem. Int. Ed. 51 (2012) 10373e10376.
[44] W. Bi, N. Leblanc, N. Mercier, P. Auban-Senzier, C. Pasquier, Chem. Mater. 21 (2009) 4099e4101.
[45] H.R. Jeon, D.W. Lee, K.M. Ok, J. Solid State Chem. 187 (2012) 83e88.
[46] M. Ranjbar, H. Aghabozorg, A. Moghimi, Z. Kristallogr, NCS 218 (2003) 432e434.

[47] H. Aghabozorg, F. Ramezanipour, J. Soleimannejad, M.A. Sharif, A. Shokrollahi, M. Shamsipur, A. Moghimi, J.A. Gharamaleki, V. Lippolis, A.J. Blake, Pol. J. Chem. 82 (2008) 487e507.
[48] S. Sheshmani, P.D. Kheirollahi, H. Aghabozorg, A. Shokrollahi, G. Kickelbick, M. Shamsipur, F. Ramezanipour, A. Moghimi, Z. Anorg. Allg. Chem. 631 (2005) 3058e3065.
[49] M.A. Sharif, H. Aghabozorg, A. Moghimi, Acta Crystallogr. E63 (2007) m1599em1601.

[50] V. Stavila, K.H. Whitmire, I. Rusakova, Chem. Mater. 21 (2009) 5456e5465.
[51] V. Stavila, I. Bulimestru, A. Gulea, A.C. Colson, K.H. Whitmire, Acta Crystallogr. C67 (2011) m65em68.
[52] Bruker, SAINTPlus, V. 6.2. Data Reduction and Correction Program, Bruker AXS, Madison, Wisconsin, USA, 2001.
[53] Bruker, APEX2 Software Package, V. 1.27. Bruker Molecular Analysis Research Tool, Bruker AXS, Madison, Wisconsin, USA, 2005.
[54] Oxford Diffraction Ltd, Abingdon (UK)..
[55] CrysAlisPro, Agilent Technologies, Version 1.171.36.20 (release 27-06-2012 CrysAlis171.NET, compiled Jul 11 2012, 15:38:31).
[56] G.M. Sheldrick, Acta Crystallogr. A64 (2008) 112e122.
[57] C.F. Macrae, I.J. Bruno, P.R. Chrisholm, P.R. Edgington, P. McCabe, E. Pidcock, L. Rodriguez-Monge, R. Taylor, J. van de Steek, P.A. Wood, J. Appl. Crystallogr. 41 (2008) 466e470. http://www.ccdc.cam.ac.uk/mercury/.
[58] M.J. Nardelli, J. Appl. Crystallogr. 28 (1995) 659e673.
[59] L.J. Farrugia, WINGX (ver. 1.80.05), J. Appl. Crystallogr. 32 (1999) 837e838.
[60] B.-M. Kukovec, G.A. Venter, G.L. Oliver, Cryst. Growth Des. 12 (1) (2012) 456e465.

[61] K. Nakamoto, Infrared and Raman Spectra of Inorganic and Coordination Compounds, Part B, sixth ed., John Wiley & Sons, Hoboken, 2009 New York, 1963.

[62] G.B. Deacon, R. Phillips, J. Coord. Chem. Rev. 33 (1980) 227e250.
[63] F.H. Allen, Acta Crystallogr. B58 (2002) 380e388.
[64] I.D. Brown, Chem. Soc. Rev. 7 (1978) 359e376.
[65] I.D. Brown, D. Altermatt, Acta Crystallogr. B41 (1985) 244e247.
[66] I.D. Brown, The Chemical Bond in Inorganic Chemistry: the Bond Valence Model, Oxford Univ. Press, New York, 2002.
[67] D. Massiot, S. Drumel, P. Janvier, M. Bujoli-Doeuff, B. Bujoli, Chem. Mater. 9 (1997) 6e7.